




Ligand-modulated aqueous synthesis of color-tunable copper nanoclusters for the photoluminescent assay of Hg(II)

Mingxia Jiao¹ · Yun Li¹ · Yuxiu Jia¹ · Le Xu¹ · Guiyun Xu¹ · Yingshu Guo² · Xiliang Luo¹ 

Received: 13 July 2020 / Accepted: 28 August 2020 / Published online: 4 September 2020
© Springer-Verlag GmbH Austria, part of Springer Nature 2020

Abstract

Water-soluble Cu nanoclusters (NCs) with tunable emission were synthesized through an eco-friendly one-pot aqueous method. Blue-, green-, and red-emitting NCs with the emission peaks at 420 nm, 505 nm, and 630 nm were obtained by employing ethanediamine, cysteine, and glutathione as surface ligands, respectively. The ligand effects on the optical properties of Cu NCs were studied by the single variable method. It has been revealed by systematic characterizations that the dependence of emission color on the structures of ligands was mainly attributed to their different size-tuning effects. Glutathione has the strongest chelating ability and it can significantly reduce the monomer reactivity and thus decrease the supersaturation degree of the reaction, which is favorable for modulating Cu precursor to grow into larger NCs. In contrast, ethanediamine ligand resulted in smaller nanoclusters due to its weaker binding capability. Because of the strong emission and terrific fluorescent stability, Cu NCs capped with ethanediamine, possessing an emission peak at 420 nm when excited at a wavelength of 350 nm, were directly used for probing Hg(II) with satisfying selectivity, presenting a linear range of 0.1–5.0 mM and a detection limit of 33 μ M. The sensor showed good performance in real sample analysis with recoveries ranging from 99% to 103%, and comparable accuracy with atomic fluorescence spectroscopy, manifesting the reliability of the current strategy for sensing Hg(II).

Keywords Copper nanoclusters · Aqueous synthesis · Ligand effects · Tunable emission · Metal ion assay

Electronic supplementary material The online version of this article (<https://doi.org/10.1007/s00604-020-04539-6>) contains supplementary material, which is available to authorized users.

✉ Yingshu Guo
yingshug@126.com

✉ Xiliang Luo
xiliangluo@qust.edu.cn

¹ Key Laboratory of Optic-electric Sensing and Analytical Chemistry for Life Science, MOE, Shandong Key Laboratory of Biochemical Analysis, Key Laboratory of Analytical Chemistry for Life Science in Universities of Shandong, College of Chemistry and Molecular Engineering, Qingdao University of Science and Technology, Qingdao 266042, China

² Collaborative Innovation Center of Tumor Marker Detection Technology, Equipment and Diagnosis-Therapy Integration in Universities of Shandong, Shandong Province Key Laboratory of Detection Technology for Tumor Markers, School of Chemistry and Chemical Engineering, Linyi University, Linyi 276005, China

Introduction

Metal nanoclusters (NCs), which are tiny colloidal nanoparticles composed of a few to some hundreds of metal atoms, show great potential in the biomedical field, optoelectronics, and sensor development as supplements to molecular level phosphors and luminescent semiconductor nanocrystals, due to their small size, biocompatibility, large Stokes shift, and reasonably strong photoluminescence (PL) [1–5]. Compared with conventional noble Au and Ag NCs, copper NCs display the advantages of earth-abundant precursors, relatively low-cost, and rich surface chemistry [6–8].

Inspired by their unique molecule-like optical properties and subsequent application prospect, the synthesis of Cu NCs has gained growing research interest in the past decade [2, 9–15]. As they suffer from easy oxidation in air and aggregation during the preparation process, appropriate stabilizing agents are indispensable for achieving stable Cu NCs. Up to now, various surface ligands including DNA, proteins, peptides, polymers, and small molecules have been employed to synthesize Cu NCs [16–22]. Recently, small molecules

especially thiol-containing molecules have been widely used, because they can serve as both capping ligand and reductant and are convenient to use under mild conditions and much lower cost compared with the others [10, 23, 24]. For example, Li et al. developed a special strategy for the fast fabrication of red-emitting Cu NCs with the assistance of green-emitting Cu NCs in the presence of dihydrolipoic acid (DHLA) as a protecting ligand and bis[tetrakis(hydroxymethyl)phosphonium] sulfate (THPS) as a reducing agent, maintaining the water solubility and tiny size of the NCs [25]. Wang and coworkers prepared self-assembled Cu NCs by mixing tetrafluorothiophenol (TFTP) with a copper source in ethanol, which exhibited intense saffron yellow (590 nm) PL via self-assembly-induced emission [1]. Zhao et al. prepared hydrophobic 4-methylthiophenol-capped Cu NCs and stable aggregation-induced emission particles with intense red luminescence via self-assembly mediated by the hydrophobic interaction [26]. Wang et al. reported two Cu NCs stabilized by L-cysteine and glutathione which exhibited green and red emission respectively [10]. Zhang group prepared Cu NC self-assembled ribbons with tunable emission in a range of 548 to 698 nm by employing aromatic thiols with different substituent groups and substituent positions as the capping ligands [27]. Das et al. used glutathione as the surface ligand to prepare glutathione-capped Cu NCs in alkaline solution under 40 °C and 14 h of vigorous stirring [28]. Despite the above achievements, there remains a lack of a systematic study about the surface ligand effect on the optical properties of Cu NCs, which has been intensively investigated for Au and Ag NCs [5, 29, 30]. On the other hand, for achieving color-tunable Cu NCs and assembly, most of the preparation routes are based on the non-aqueous phase synthesis, and the resulting hydrophobic particles are not compatible with biological systems before further surface modification. There already exist some reports of small molecule-capped Cu NCs via aqueous synthesis [10, 23, 24, 31], but many of them suffered from tedious and time-consuming processes. Therefore, it is necessary to develop cost-effective synthetic methods and explore the surface ligand effect for achieving water-soluble Cu NCs with tunable PL.

Following our previous studies on preparation and sensing applications of Cu-based nanocrystals and noble metal NCs and ligand effects on iron oxide nanocrystals [32–36], herein, we report an aqueous synthesis of Cu NCs with tunable emission by employing small molecules with different functional groups as surface ligands. The ligand effects on the PL properties were investigated by spectroscopic characterization in combination with structural and compositional analysis on the resulting NCs. Exploring mild and rapid strategy for Hg²⁺ determination is highly demanded due to its toxicity, and the commonly used elemental analysis methods such as atomic fluorescence spectrometry (AFS) suffer from rigorous and time-consuming. The prepared Cu NCs selectively exhibited

decreased PL towards Hg(II), even in the presence of various interferences.

Material and methods

Chemicals

Copper sulfate pentahydrate (CuSO₄·5H₂O, ≥ 99.0%, Tianjin Bodi Chemical Co. Ltd., <https://bdhg.company.lookchem.cn/>), reduced L-glutathione (GSH, ≥ 98.0%, Aldrich, <https://www.sigmaaldrich.com/>), L-cysteine (Cys, 99%, Aladdin, <http://www.aladdin-e.com/>), ethanediamine (EDA, ≥ 99.0%, Aldrich, <https://www.sigmaaldrich.com/>), and ascorbic acid (AA, AR, Sinopharm Chemical Reagent Co. Ltd., <http://www.sinoreagent.com/>) were used as received. Other reagents including HCl solution (12 mol/L) and acetone of analytical reagent from Yantai Far East Fine Chemical Co. Ltd. (<http://191131.biochemsafebuy.com/>), ethanol of analytical reagent from Sinopharm Chemical Reagent Co. Ltd. (<http://www.sinoreagent.com/>), and NaOH of analytical reagent from Aladdin (<http://www.aladdin-e.com/>) were used as received without further purification. Mercury perchlorate trihydrate (Hg(ClO₄)₂·3H₂O), NaCl, NaNO₃, Na₂SO₄, AgNO₃, PbCl₂, CdCl₂, BaCl₂, NiCl₂, CoCl₂, MgCl₂, MnCl₂, and CuCl₂ of analytical reagent from Aladdin (<http://www.aladdin-e.com/>) is used as received. Millipore ultra-pure water (Milli-Q water) (resistivity is 18.2 MΩ·cm) was utilized throughout the experiments.

Synthesis of water-soluble Cu NCs

Typically, for synthesizing Cu NCs with blue PL, CuSO₄·5H₂O (0.0800 mmol), EDA (1.36 mmol), and AA (0.800 mmol) were dissolved into 24-mL ultrapure water in a 50-mL flask under magnetic stirring to form a homogeneous solution with the pH value kept at about 4.5 using 1 M NaOH. The resultant solution was then heated to 37 °C and kept for a certain reaction time. Afterwards, the solution was cooled to room temperature. The resultant nanoclusters were precipitated by 2-propanol (volume ratio of 2-propanol and sample solution: 3:1), collected by centrifugation at 4000 rpm for 10 min, washed with 2-propanol (volume ratio of 2-propanol and added water: 3:1) for three cycles, and finally redispersed in water for further experiments. For synthesizing Cu NCs with green and red PL, EDA was replaced by the same amount of Cys and GSH respectively, while the other reaction conditions were maintained the same.

Spectroscopic characterization

Steady-state UV–Vis absorption and PL spectra were recorded at room temperature on a Shimadzu UV-2600 UV–Vis

spectrophotometer and a Hitachi F-4600 fluorescence spectrophotometer, respectively. The optimal excitation wavelengths for steady-state PL measurements were as follows: 350 nm for the Cu NCs capped with EDA, and 420 nm and 370 nm for NCs capped with Cys and GSH ligand respectively. Time-resolved PL decay measurement was carried out on an Edinburgh Instruments FLS980 spectrometer equipped with a picosecond pulsed diode laser (EPL-360) as a single wavelength excitation source. The absolute PL QY of the NCs was determined by a Binsong c1515947s spectrometer with the excitation wavelength of 350 nm. The fluorescent stability of the as-prepared Cu NCs along with placing time and pH was monitored by a Hitachi F-4600 fluorescence spectrophotometer.

Structural and compositional characterization

Transmission electron microscope (TEM) and high-resolution TEM (HRTEM) images of the QDs were taken on a JEM-2100F electron microscope at an acceleration voltage of 200 kV. The particle size was determined by averaging at least 300 particles per sample by ImageJ. The Fourier transform infrared (FTIR) spectra were recorded on a Nicolet iS 10 spectrophotometer (Germany) in the range of 4000–900 cm^{-1} . X-ray photoelectron spectroscopy (XPS) measurements were carried out with a Thermo-VG Scientific ESCALAB 250Xi spectrometer with a monochromatic Al $K\alpha$ X-ray source.

Performance of Hg^{2+} determination

For Hg^{2+} determination, a series of Hg^{2+} aqueous solutions were separately mixed with the aqueous solution of EDA-capped Cu NCs at pH 6, and the Hg^{2+} concentration in the final solution was 0.1, 0.2, 0.3, 0.4, 0.5, 0.6, 0.8, 1, 2, 3, 4, and 5 mM respectively. The mixture was incubated at room temperature for 10 min and then the fluorescence emission spectra were recorded with the excitation wavelength of 350 nm. When measuring the fluorescence of Cu NCs in the presence or absence of Hg^{2+} in different pH environments, phosphate-buffered saline (PBS) with a pH value from 2 to 8 was used respectively. Apart from Hg^{2+} , various metal ions including Na^+ , Ag^+ , Pb^{2+} , Cd^{2+} , Ba^{2+} , Ni^{2+} , Co^{2+} , Mg^{2+} , Mn^{2+} , and Cu^{2+} and anions including ClO_4^- , Cl^- , OH^- , NO_3^- , and SO_4^{2-} were adopted in the selectivity experiments, and the individual concentration of all the ions was set to 1.0 mM. The treatment processes were the same as those for Hg^{2+} determination as stated above. For the real sample detection, the tap water was used directly for Hg^{2+} assay by recovery experiments. The added Hg^{2+} concentrations were 0.5 mM, 1.0 mM, and 2.5 mM respectively. For assessing the accuracy of the current method, the water samples were also tested by

the atomic fluorescence spectrometry (AFS) method (instrument model: XGY 1011A).

Results and discussion

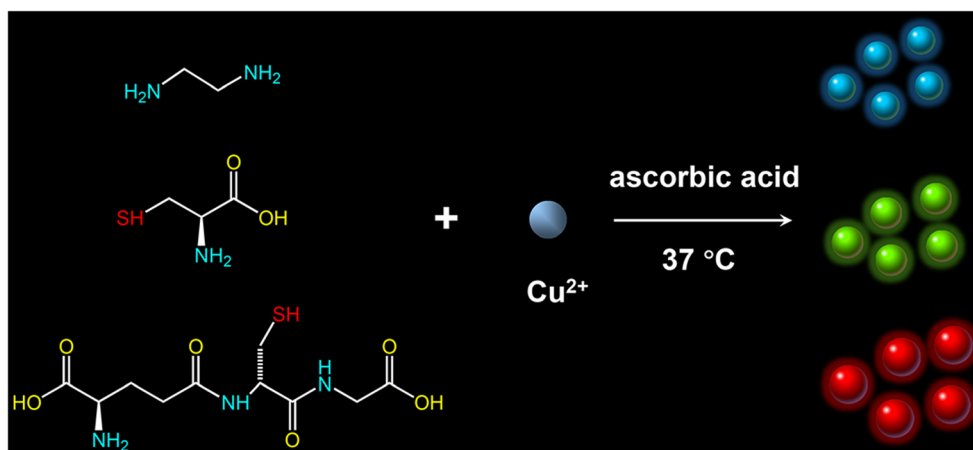
Influence of surface ligand on optical properties of water-soluble Cu NCs

The water-soluble Cu NCs were synthesized in water at 37 °C employing CuSO_4 as the metal precursor and ascorbic acid as the reduction agent in the presence of different surface ligands, as described in the “Material and methods” section. It is important to note that the reaction conditions including metal precursor, reduction agent, pH value, and reaction temperature for all samples were kept constant to ensure comparability. In order to study the impact of surface ligand on the optical properties of Cu NCs, ethanediamine (EDA), L-cysteine (Cys), and L-glutathione (GSH) were selected as the surface ligands for each preparation (Scheme 1). As shown in Fig. 1a, blue-, green-, and red-emitting Cu NCs were obtained respectively. To achieve NCs with the brightest PL, the reaction process was monitored and a series of aliquots were extracted at different reaction time. As shown in Fig. S1b, 10 min of reaction led to a remarkable enhancement of the PL of blue-emitting NCs, and the PL reached the strongest at 40 min. Meanwhile, the absorption spectra in Fig. S1a showed the same variation tendency. For the NCs capped with Cys and GSH, the reaction time of 30 min and 20 min was needed for achieving the highest PL intensity (Fig. S1c-f). In the UV–Vis spectra shown in Fig. 1b, one well-resolved absorption peak appears at 340 nm for EDA-capped Cu NCs, while for Cys- and GSH-capped NCs, the absorption peaks are rather structureless. In contrast, well-resolved peaks at 350 nm, 420 nm, and 370 nm are observed in the photoluminescence excitation (PLE) spectra (Fig. S2) for the blue-, green-, and red-emitting NCs. Figure 1c presents the normalized PL spectra of the three Cu NCs, with the emission peaks locating at 420 nm, 505 nm, and 630 nm respectively. The full width at half-maximum (FWHM) are 57 nm, 89 nm, and 110 nm for the three NCs. Among the three Cu NCs, the EDA-capped Cu NCs possess the highest PL intensity, as presented in Fig. S3.

Influence of surface ligand on compositional and structural properties

The valence state of the prepared Cu NCs was analyzed by X-ray photoelectron spectroscopy (XPS). As shown in Fig. 2a, all the NCs present two peaks at 932 eV and 952 eV in the high-resolution XPS spectra irrespective of the surface ligand, which are assigned to $2p_{3/2}$ and $2p_{1/2}$ states of metallic Cu [7]. The reduction of Cu^{2+} by ascorbic acid is evidenced by the absence of any satellite peaks around 942 eV. It is worth

Scheme 1 Schematic illustration of aqueous synthesis of Cu NCs capped with ethanediamine, cysteine, and glutathione respectively



mentioning that the difference in binding energy between $2p_{3/2}$ peaks of Cu^0 and Cu^+ species is only 0.1 eV, so the valence state of Cu in the NCs may lie between zero (in the core) and one (on the nanocrystal surface), which is consistent with previous reports [11, 12].

Furthermore, the surface bonds of Cu NCs were characterized using Fourier-transform infrared (FTIR) spectroscopy. As shown in Fig. 2b, the broad peaks between 3550 and 3300 cm^{-1} were attributed to stretching of the amino group (NH_2) existed on the surface of Cys- and GSH-capped Cu

NCs, while for EDA-coated NCs, the above peak is not evident, suggesting that EDA is connected with the Cu core through NH_2 . The peak between 2660 and 2550 cm^{-1} , which corresponds to the S–H stretching vibration mode of Cys and

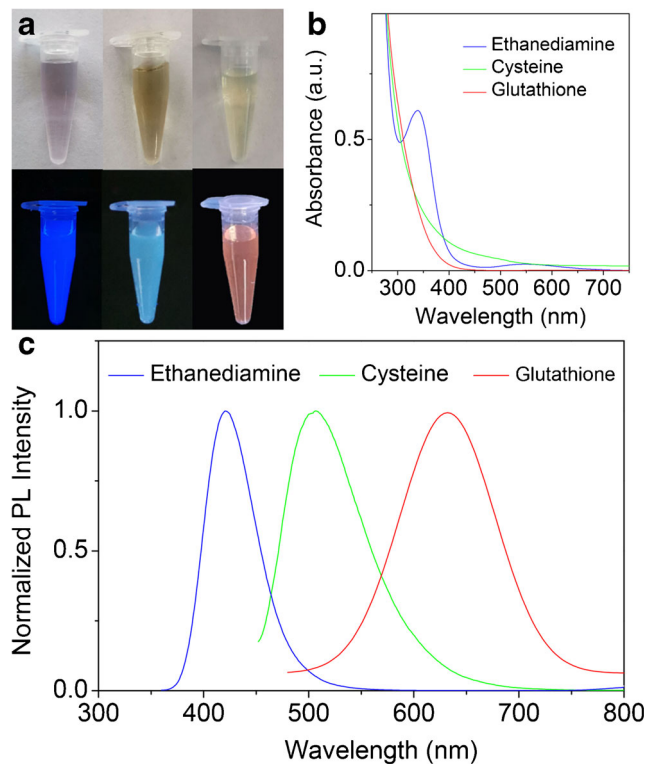


Fig. 1 Photographs of Cu NCs capped with ethanediamine, cysteine, and glutathione from left to right under room light (upper row) and 365 nm UV irradiation (lower row) (a), UV–Vis absorption (b), and normalized PL (c) spectra of Cu NCs. The excitation wavelengths were 350 nm, 420 nm, and 370 nm for three Cu NCs respectively

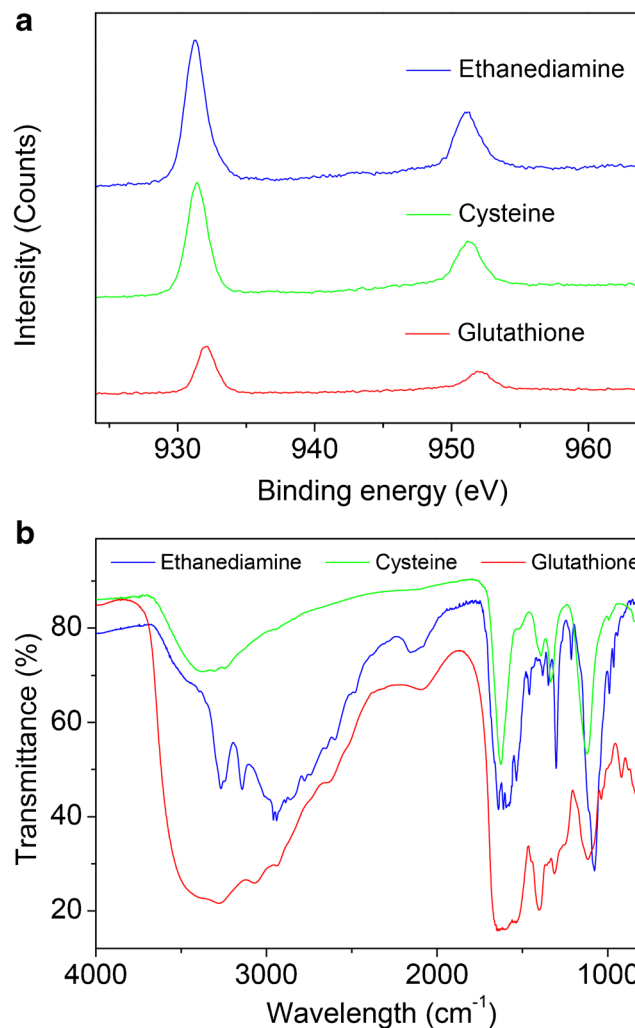


Fig. 2 X-ray photoelectron spectra (a) and Fourier-transform infrared spectra (b) of Cu NCs with different surface ligands

GSH molecules, was not found in the corresponding spectra, indicating that for the Cys- and GSH-capped NCs, thiols of the ligands may form covalent bonds to metal atoms [11, 23].

Since the synthetic conditions for obtaining the blue-, green-, and red-emitting Cu NCs were maintained the same except for the ligand species, it is clear that the ligands are key factors for the nucleation and growth processes during the reaction to form different emitted NCs. To study the morphology variations when changing the surface ligand, transmission electron microscope (TEM) measurements of the QDs were performed and the images are shown in Fig. 3. It was observed that Cu NCs were mainly distributed in the range of 2–3.4 nm with an average diameter of 2.6 nm for EDA-capped particles (Fig. 3a–b). While for Cys- and GSH-coated NCs, the average particle size was increased to 3.0 ± 0.3 nm (Fig. 3c–d) and 4.4 ± 0.5 nm (Fig. 3e–f) respectively. This suggests that in the current reaction system, the GSH ligand can modulate the Cu precursor to grow into larger NCs. During the particle formation processes, ligands coordinate to the particle surface to prevent aggregation. On the other hand, ligands can also coordinate with the Cu monomer, which can change its

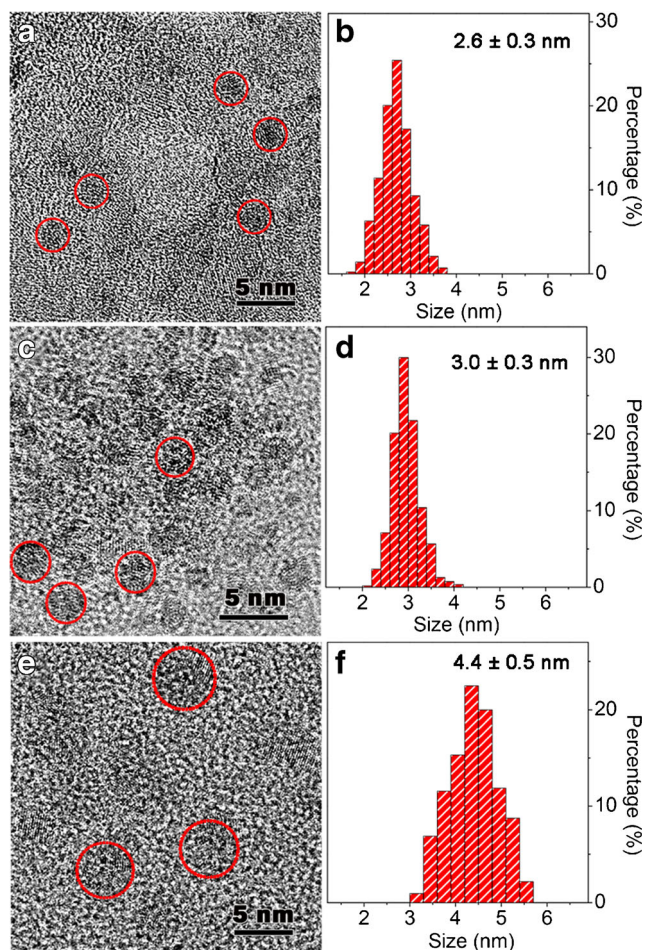


Fig. 3 Transmission electron microscope images and size histograms of Cu NCs capped with ethanediamine (a, b), cysteine (c, d), and glutathione (e, f)

reactivity. Since EDA has only the amine group to bind with Cu, while Cys possesses thiol group, amine group, and carboxyl group to coordinate with Cu precursor, and GSH also has the above three functional groups but with more quantities, the reactivity of the monomer was reduced furthest by GSH due to its strongest binding effect [32]. From a thermodynamics aspect, the supersaturation degree of the reaction decreased consequently, which is favorable for growing larger particles out of the reaction system, owing to the reduced number of nuclei generated during the nucleation process [37]. The PL of Cu NCs is known to be strongly dependent on the particle size; therefore, employing GSH as surface ligand led to large Cu NCs with red fluorescence, while EDA and Cys tend to form NCs with shorter wavelength emission.

Photoluminescence lifetime and fluorescent stability of Cu NCs

Since the EDA-capped Cu NCs possess the highest PL intensity, they were chosen as representative samples to study the transient PL property and fluorescent stability. As shown in Fig. 4a, the PL decay curve of blue-emitting NCs can be fitted by a two-exponential function: $I(t) = B_1 \exp\left(-\frac{t}{\tau_1}\right)$

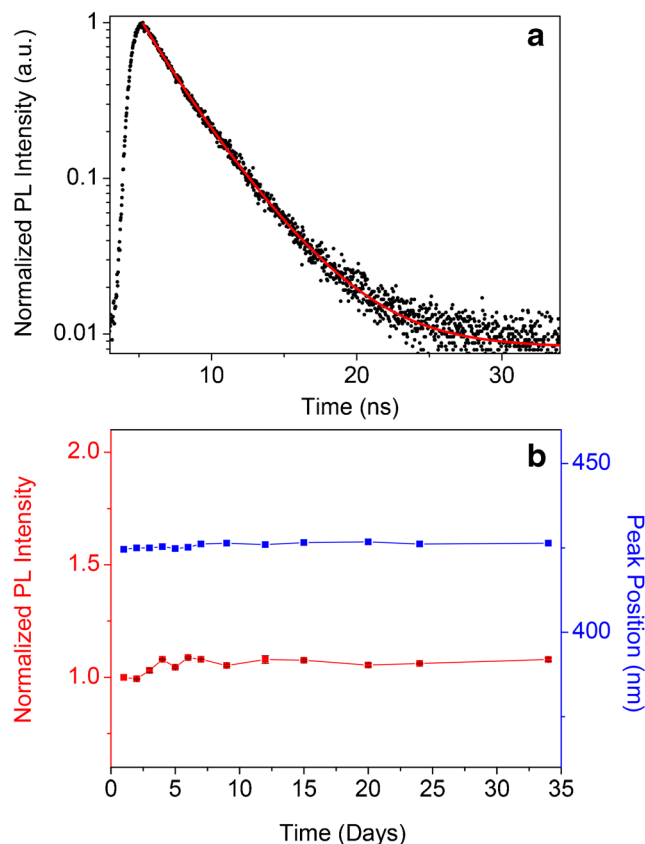


Fig. 4 Normalized time-resolved PL decay curve (a) and the temporal evolutions of the PL intensity and PL peak of Cu NCs with ethanediamine as a surface ligand (b)

$+B_2 \exp\left(-\frac{t}{\tau_2}\right)$, where τ_1 and τ_2 represent the decay time constants of the PL mission and B_1 and B_2 represent the normalized amplitudes of each component. Two components of 2.1 ns (28.4%) and 3.7 ns (71.6%) were obtained, providing an average PL lifetime of 3.6 ns. Such short PL lifetime can be attributed to the emission from the singlet excited state of metal core, as has been previously observed for blue-emitting Cu NCs [3]. The fluorescent stability of metal NCs is a key concern for their practical application, to assure the reliability of the signal.

As shown in Fig. 4b, the NCs stabilized by EDA possess terrific fluorescent stability against long placing time until 34 days, manifesting as both nearly unchanged PL peak position and intensity. This lays a solid foundation for the following sensing application of the as-prepared Cu NCs.

Performance of Hg^{2+} determination

Mercury, as one of the most toxic heavy metal pollutants, widely exists in water, soil, and foodstuffs [38–43]. In view of its toxicity, exploring effective strategies for Hg^{2+} determination is highly demanded. Based on the above-prepared blue-emitting Cu NCs with high PL intensity and stability, a fluorescent sensor for Hg^{2+} determination was developed through a mild and rapid way. Before the prepared Cu NCs were applied for assaying Hg^{2+} , repetitive ultrafiltration was performed for removing the influence of excessive ethanediamine and assuring the same background. During the assaying process, the pH of the buffer will significantly influence the sensitivity. Therefore, the pH value of the assay was optimized as shown in Fig. S4. It turned out that a nearly neutral medium facilitates the decrease of relative PL intensity, with a maximum decrease obtained at the pH 6.0. The weak acid environment can effectively reduce the protonation of the amine group on the surface of Cu NCs which would hinder the binding of Hg^{2+} , while alkaline solution would accelerate the hydrolysis of Hg^{2+} .

Figure 5a presents the PL changes of Cu NCs (with an emission peak at 420 nm excited by the wavelength of 350 nm) by introducing different concentrations of Hg^{2+} (0.1–5 mM) within 10 min at room temperature and optimal pH value of 6.0. It is evident that the PL intensity continuously decreased along with the increase of Hg^{2+} concentration, and the PL of NCs was quenched by more than 90% upon the addition of 5 mM Hg^{2+} . Apart from the change of PL intensity, the PL peak position red-shifted from 425 to 437 nm at high Hg^{2+} concentration (> 1 mM). This red-shift of PL peak may be correlated with the change of nanocluster surface state which resulted from the binding between Hg^{2+} and the amine group. To explore the mechanism of Hg^{2+} -induced fluorescence quenching of EDA-capped Cu NCs, UV–Vis absorption spectra of EDA and EDA-capped Cu NCs before and

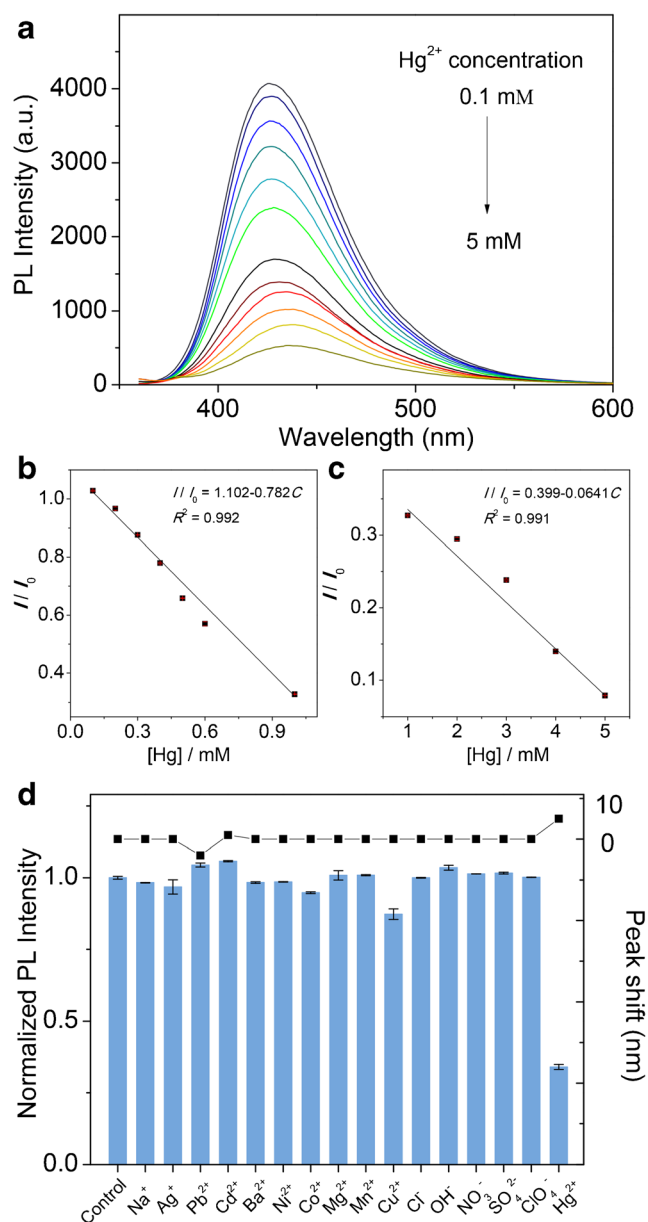


Fig. 5 PL spectra of Cu NCs capped with ethanediamine in the presence of different amounts of Hg^{2+} ions (0.1–5 mM) with an excitation wavelength of 350 nm (a), linear calibration with the standard deviation of three repeated measurements as the error bar (b, c), and normalized PL intensity (with error bars calculated from three parallel measurements) and peak shift towards low energy region of Cu NCs in the absence or presence of different ions with the concentration of 1 mM (d)

after the addition of Hg^{2+} were further investigated. As shown in Fig. S5, the Cu NCs have a well-resolved absorption peak at 340 nm (curve b), which is remarkably different from that of the surface ligand EDA (curve a, structureless absorption above 300 nm). While in the presence of Hg^{2+} , the characteristic peak of Cu NCs at 340 nm disappeared (curve c), presenting similar absorption compared with that of EDA with Hg^{2+} (curve d). It means that ethanediamine has a stronger

coordination affinity with Hg^{2+} to form stable Hg-EDA complex, which induces the fluorescence quenching of Cu NCs.

The performance of Hg^{2+} sensing was quantitatively shown in Fig. 5b and c. The relative PL intensity of Cu NCs with an emission peak at 420 nm shows a good linear relationship with Hg^{2+} concentration in two ranges: from 0.1–1.0 mM with R^2 of 0.992 (linear equation: $I/I_0 = 1.102 - 0.782C$) and from 1.0–5.0 mM with R^2 of 0.991 (linear equation: $I/I_0 = 0.399 - 0.0641C$). The detection limit was calculated to be 33 μM ($S/N = 3$). The analytical performance of the obtained Cu NCs towards Hg^{2+} is not superior compared with previous reports as shown in Table S1, which would hinder the application for trace detection. Nevertheless, the assay is mild, rapid, and low-cost, and most importantly, the Cu NCs can be directly used as the sensing probe without further modification, which is suitable for the fast assay of Hg^{2+} .

To assess the selectivity of Cu NCs for Hg^{2+} , the PL spectra of NCs were measured in the presence of other ten metal ions including Na^+ , Ag^+ , Pb^{2+} , Cd^{2+} , Ba^{2+} , Ni^{2+} , Co^{2+} , Mg^{2+} , Mn^{2+} , and Cu^{2+} , and anions including Cl^- , OH^- , NO_3^- , SO_4^{2-} , and ClO_4^- . As shown in Fig. 5d, the relative PL intensities of the NCs generally exhibit no significant changes upon the above ions compared with Hg^{2+} under the same ion concentration, even in the presence of commonly existing heavy metal ions such as Cu^{2+} , Pb^{2+} , and Cd^{2+} . Since the fluorescence quenching mechanism of Cu NCs towards Hg^{2+} is the greater coordination affinity of Hg^{2+} with ethanediamine, the weak response of Cu NCs to other metal ions can be attributed to their weaker combining capability with ethanediamine, which is not strong enough to grab the surface ligand of Cu NCs. For example, the formation constants ($\log K_1$) of Cu(II)-EDA and Cd(II)-EDA complexes are 10.67 and 5.47 respectively, while that of Hg(II)-EDA is 14.3 [44]. More importantly, the presence of possible interfering ions can hardly shift the PL peak position of the Cu NCs except that Pb^{2+} caused a blue-shift of about 4 nm, while Hg^{2+} resulted in a red-shift of about 5 nm. The fluorescence spectra with different emission peaks further ensure the selectivity. Therefore, the interfering ions have nearly no influence on the sensing capability of the Cu NCs for Hg^{2+} determination. Furthermore, the Cu NCs were applied to assay Hg^{2+} in tap water. As shown in Table S2, the recovery rates were 100.5%, 99.46%, and 103.4% with RSD values of less than 4.9% for three samples, revealing good potential of the current method for sensing Hg^{2+} in real samples. To further prove the accuracy of the assay, water samples were also tested by the atomic fluorescence spectrometry (AFS) method. The results in Table S2 show that our method and AFS have comparable accuracy, demonstrating the reliability of the method for sensing Hg^{2+} . However, the sensitivity of the developed method based on Cu NCs needs to be improved for trace detection in real samples.

Conclusions

Water-soluble Cu NCs with blue, green, and red emissions were synthesized by choosing ethanediamine, cysteine, and glutathione as surface ligands respectively. The formation of Cu NCs supported by the above ligands was confirmed by XPS, FTIR, and TEM characterizations. The dependence of emission color on the structures of ligands was mainly attributed to their different chelating ability, which can greatly affect the supersaturation degree of monomers bound to ligands. As a consequence, NCs with different sizes were formed and exhibited different emission wavelengths due to the size effect. Without further surface modification, Cu NCs capped with ethanediamine were directly employed as the probe for mild and rapid sensing of Hg^{2+} with satisfying selectivity. The fluorescence quenching mechanism was mainly attributed to the strong coordination affinity of Hg^{2+} with ethanediamine. Because the Cu element is low-toxic and earth-abundant, the current work of tuning the emission color of Cu NCs by ligand effect has provided an effective approach towards NCs with controlled properties and potentially scaling up capacity. Nevertheless, the sensitivity of the assay needs to be further improved for trace detection of Hg(II), which can find new ways by combining with other functional nanomaterials.

Acknowledgments The authors would like to acknowledge the financial support from the Natural Science Foundation of China (NSFC, 21802083, 21974075) and the Taishan Scholar Program of Shandong Province of China (ts20110829).

Compliance with ethical standards

Conflict of interest The authors declare that they have no competing interests.

References

1. Han A, Xiong L, Hao S, Yang Y, Li X, Fang G, Liu J, Pei Y, Wang S (2018) Highly bright self-assembled copper nanoclusters: a novel Photoluminescent probe for sensitive detection of histamine. *Anal Chem* 90:9060–9067
2. Ye M, Yu Y, Lin B, Cai Y, Cao Y, Guo M, Zhu D (2019) Copper nanoclusters reversible switches based on ions-triggered for detection of inorganic pyrophosphatase activity. *Sensors Actuators B Chem* 284:36–44
3. Wang Z, Chen B, Rogach AL (2017) Synthesis, optical properties and applications of light-emitting copper nanoclusters. *Nanoscale Horiz* 2:135–146
4. Hu X, Liu T, Zhuang Y, Wang W, Li Y, Fan W, Huang Y (2016) Recent advances in the analytical applications of copper nanoclusters. *TrAC Trend Anal Chem* 77:66–75
5. Zhang L, Wang E (2014) Metal nanoclusters: new fluorescent probes for sensors and bioimaging. *Nano Today* 9:132–157
6. Zhou T, Zhu J, Gong L, Nong L, Liu J (2019) Amphiphilic block copolymer-guided in situ fabrication of stable and highly controlled

- luminescent copper Nanoassemblies. *J Am Chem Soc* 141:2852–2856
7. Wang Z, Y-e S, Yang X, Xiong Y, Li Y, Chen B, Lai W-F, Rogach AL (2018) Water-soluble biocompatible copolymer hyppromellose grafted chitosan able to load exogenous agents and copper nanoclusters with aggregation-induced emission. *Adv Funct Mater* 28:1802848
 8. Hu X, Liu X, Zhang X, Chai H, Huang Y (2018) One-pot synthesis of the CuNCs/ZIF-8 nanocomposites for sensitively detecting H₂O₂ and screening of oxidase activity. *Biosens Bioelectron* 105:65–70
 9. Liu Y, Yao D, Zhang H (2018) Self-assembly driven aggregation-induced emission of copper nanoclusters: a novel technology for lighting. *ACS Appl Mater Interfaces* 10:12071–12080
 10. Wang Z, Zhang CC, Gao J, Wang Q (2017) Copper clusters-based luminescence assay for tetracycline and cellular imaging studies. *J Lumin* 190:115–122
 11. Lin L, Hu Y, Zhang L, Huang Y, Zhao S (2017) Photoluminescence light-up detection of zinc ion and imaging in living cells based on the aggregation induced emission enhancement of glutathione-capped copper nanoclusters. *Biosens Bioelectron* 94:523–529
 12. Zhao M, Chen A-Y, Huang D, Zhuo Y, Chai Y-Q, Yuan R (2016) Cu nanoclusters: novel electrochemiluminescence emitters for bioanalysis. *Anal Chem* 88:11527–11532
 13. Wu Z, Liu J, Gao Y, Liu H, Li T, Zou H, Wang Z, Zhang K, Wang Y, Zhang H, Yang B (2015) Assembly-induced enhancement of Cu nanoclusters luminescence with mechanochromic property. *J Am Chem Soc* 137:12906–12913
 14. Huang Y, Liu W, Feng H, Ye Y, Tang C, Ao H, Zhao M, Chen G, Chen J, Qian Z (2016) Luminescent nanoswitch based on organic-phase copper nanoclusters for sensitive detection of trace amount of water in organic solvents. *Anal Chem* 88:7429–7434
 15. Qing T, Zhang K, Qing Z, Wang X, Long C, Zhang P, Hu H, Feng B (2019) Recent progress in copper nanocluster-based fluorescent probing: a review. *Microchim Acta* 186:670
 16. Tang Q, Yang T, Huang Y (2015) Copper nanocluster-based fluorescent probe for hypochlorite. *Microchim Acta* 182:2337–2343
 17. Liu G, Shao Y, Peng J, Dai W, Liu L, Xu S, Wu F, Wu X (2013) Highly thymine-dependent formation of fluorescent copper nanoparticles templated by ss-DNA. *Nanotechnology* 24:345502
 18. Qing Z, He X, He D, Wang K, Xu F, Qing T, Yang X (2013) Poly(thymine)-templated selective formation of fluorescent copper nanoparticles. *Angew Chem Int Edit* 52:9719–9722
 19. Jia X, Yang X, Li J, Li D, Wang E (2014) Stable Cu nanoclusters: from an aggregation-induced emission mechanism to biosensing and catalytic applications. *Chem Commun* 50:237–239
 20. Lin Y-J, Chen P-C, Yuan Z, Ma J-Y, Chang H-T (2015) The isomeric effect of mercaptobenzoic acids on the preparation and fluorescence properties of copper nanoclusters. *Chem Commun* 51:11983–11986
 21. Miao H, Zhong D, Zhou Z, Yang X (2015) Papain-templated Cu nanoclusters: assaying and exhibiting dramatic antibacterial activity cooperating with H₂O₂. *Nanoscale* 7:19066–19072
 22. Borghei Y-S, Hosseini M, Ganjali MR, Hosseinkhani S (2017) Label-free fluorescent detection of microRNA-155 based on synthesis of hairpin DNA-templated copper nanoclusters by etching (top-down approach). *Sensors Actuators B Chem* 248:133–139
 23. Wang Z, Chen B, Susha AS, Wang W, Reckmeier CJ, Chen R, Zhong H, Rogach AL (2016) All-copper nanocluster based down-conversion white light-emitting devices. *Adv Sci* 3:1600182
 24. Yang X, Feng Y, Zhu S, Luo Y, Zhuo Y, Dou Y (2014) One-step synthesis and applications of fluorescent Cu nanoclusters stabilized by L-cysteine in aqueous solution. *Anal Chim Acta* 847:49–54
 25. Li D, Wang G, Peng Y, Chen Z, Gao X, Cheng L, Mei X (2019) Development of ratiometric sensing and white light-harvesting materials based on all-copper nanoclusters. *Nanoscale Adv* 1:1086–1095
 26. Zhao M, Qian Z, Zhong M, Chen Z, Ao H, Feng H (2017) Fabrication of stable and luminescent copper nanocluster-based AIE particles and their application in β -galactosidase activity assay. *ACS Appl Mater Interfaces* 9:32887–32895
 27. Ai L, Jiang W, Liu Z, Liu J, Gao Y, Zou H, Wu Z, Wang Z, Liu Y, Zhang H, Yang B (2017) Engineering a red emission of copper nanocluster self-assembly architectures by employing aromatic thiols as capping ligands. *Nanoscale* 9:12618–12627
 28. Das NK, Ghosh S, Priya A, Datta S, Mukherjee S (2015) Luminescent copper nanoclusters as a specific cell-imaging probe and a selective metal ion sensor. *J Phys Chem C* 119:24657–24664
 29. Li J, Zhu J-J, Xu K (2014) Fluorescent metal nanoclusters: from synthesis to applications. *TrAC Trend Anal Chem* 58:90–98
 30. Luo Z, Yuan X, Yu Y, Zhang Q, Leong DT, Lee JY, Xie J (2012) From aggregation-induced emission of Au(I)-thiolate complexes to ultrabright Au(0)@Au(I)-thiolate core-shell nanoclusters. *J Am Chem Soc* 134:16662–16670
 31. Wang L, Miao H, Zhong D, Yang X (2016) Synthesis of dopamine-mediated Cu nanoclusters for sensing and fluorescent coding. *Anal Methods* 8:40–44
 32. Jiao M, Jing L, Wei X, Liu C, Luo X, Gao M (2017) The Yin and Yang of coordinating co-solvents in the size-tuning of Fe₃O₄ nanocrystals through flow synthesis. *Nanoscale* 9:18609–18612
 33. Xu S, Li W, Zhao X, Wu T, Cui Y, Fan X, Wang W, Luo X (2019) Ultrahighly efficient and stable fluorescent gold nanoclusters coated with screened peptides of unique sequences for effective protein and serum discrimination. *Anal Chem* 91:13947–13952
 34. Jiao M, Li Y, Jia Y, Yang Z, Luo X (2019) Aqueously synthesized color-tunable quaternary Cu-In-Zn-S quantum dots for Cu(II) detection via mild and rapid cation exchange. *Sensors Actuators B Chem* 294:32–39
 35. Wang Y, Cui M, Jiao M, Luo X (2018) Antifouling and ultrasensitive biosensing interface based on self-assembled peptide and aptamer on macroporous gold for electrochemical detection of immunoglobulin E in serum. *Anal Bioanal Chem* 410:5871–5878
 36. Jiao M, Huang X, Ma L, Li Y, Zhang P, Wei X, Jing L, Luo X, Rogach A, Gao M (2019) Biocompatible off-stoichiometric copper indium sulfide quantum dots with tunable near-infrared emission via aqueous based synthesis. *Chem Commun* 55:15053–15056
 37. Jiao M, Jing L, Liu C, Hou Y, Huang J, Wei X, Gao M (2016) Differently sized magnetic/upconversion luminescent NaGdF₄:Yb, Er nanocrystals: flow synthesis and solvent effects. *Chem Commun* 52:5872–5875
 38. Hu X, Wang W, Huang Y (2016) Copper nanocluster-based fluorescent probe for sensitive and selective detection of Hg²⁺ in water and food stuff. *Talanta* 154:409–415
 39. Suo Z, Hou X, Hu Z, Liu Y, Xing F, Feng L (2019) Fibrinogen-templated gold nanoclusters for fluorometric determination of cysteine and mercury(II). *Microchim Acta* 186:799
 40. Ru F, Du P, Lu X (2020) Efficient ratiometric fluorescence probe utilizing silicon particles/gold nanoclusters nanohybrid for “on-off-on” bifunctional detection and cellular imaging of mercury (II) ions and cysteine. *Anal Chim Acta* 1105:139–146
 41. Liu R, Zuo L, Huang XR, Liu SM, Yang GY, Li SY, Lv CY (2019) Colorimetric determination of lead(II) or mercury(II) based on

- target induced switching of the enzyme-like activity of metallothionein-stabilized copper nanoclusters. *Microchim Acta* 186:250
42. Mao A, Wei C (2019) Cytosine-rich ssDNA-templated fluorescent silver and copper/silver nanoclusters: optical properties and sensitive detection for mercury(II). *Microchim Acta* 186:541
 43. Lin SM, Geng S, Li N, Li NB, Luo HQ (2016) D-penicillamine-templated copper nanoparticles via ascorbic acid reduction as a mercury ion sensor. *Talanta* 151:106–113
 44. Dean JA (1999) *Lange's handbook of chemistry*, 15th edn. McGraw-Hill, New York

Publisher's note Springer Nature remains neutral with regard to jurisdictional claims in published maps and institutional affiliations.